ISSN : 0974 - 7486 Volume 10 Issue 4

Trade Science Inc.

Materials Science

An Indian Journal

Full Paper

MSAIJ, 10(4), 2014 [152-159]

Thermodynamic study, elaboration and high temperature oxidation of alloys highly strengthened by tantalum carbides. Part 1: Case of a Co-30Cr-1C-15Ta alloy

Laura Corona[1,3], Patrice Berthod[2,3]*
[1]Faculty of Sciences and Technologies, B.P. 70239, 54506 Vandoeuvre-lès-Nancy – (FRANCE)
[2]Institut Jean Lamour (UMR 7198), Team 206 "Surface and Interface, Chemical Reactivity of Materials"
B.P. 70239, 54506 Vandoeuvre-lès-Nancy – (FRANCE)
[3]University of Lorraine, F.S.T., B.P. 70239, 54506 Vandoeuvre-lès-Nancy – (FRANCE)
E-mail : Patrice.Berthod@univ-lorraine.fr

ABSTRACT

Many alloys designed for wear resistance are composed of a metallic matrix and a high fraction of carbides. When the matrix is based on cobalt there are often chromium carbides or tungsten carbides which play the role of hard phases. In this work a new alloy, based on cobalt and rich in chromium, elaborated by foundry and wished to contain great fraction of another type of carbide: TaC, was considered. With high amounts in both carbon and tantalum, respectively 1 wt.% and 15 wt.%, great volume fractions in tantalum carbides were obtained. Most of them are script-like eutectic carbides situated in the interdendritic spaces, a microstructure feature known to be favourable to general mechanical resistance at high temperature, and additional compact TaC carbides were also present. The obtained hardness is of a good level (about 440 Hv_{30kg}) and the resistance to high temperature oxidation, evaluated during 46 hours at 1150°C, was good with an obvious chromia-forming behaviour and the development of only a limited carbide-free zone from the surface.

KEYWORDS

Cobalt alloys;
Tantalum carbides;
Thermodynamic calculations;
Microstructures;
Hardness;
High temperature oxidation.

INTRODUCTION

Chromium-rich cobalt-based alloys can be encountered in many applications, from cryogenic/ambient/body temperatures, as prosthetic dentistry[1], up to very high temperatures (e.g. aero-engines[2], industrial processes[3]), where corrosion resistance in corrosive aqueous milieus or resistance against high temperature oxidation by gases or hot corrosion by molten salts or CMAS glasses are required[4]. Many of them also contain carbon which allows the development of carbides useful for high mechanical resistance at high temperature (e.g. for combating creep deformation)[5]. Some versions especially rich in carbon and highly alloyed with carbides-former elements can be used to take benefit from the intrinsic rather high hardness of cobalt and the high hardness of carbides, for example as cutting tools[6] made of a cobalt matrix hardened with high amounts of dispersed tungsten carbides, or for Co-W_2C coatings[7] for improving wear resistance of some metallic alloys.

High densities of carbides can be obtained in alloys elaborated by foundry, as the very great fractions of chromium carbides recently obtained in ternary chromium-rich cobalt-based alloys[8].

Besides tungsten or chromium other elements can be considered to develop carbides in great quantities, as the MC-formers ones: Ta, Hf, Zr... In this study it the case of tantalum which was selected. For obtaining only MC carbides (tantalum is a carbide-former element stronger than chromium), taking into consideration that another carbide-forming element – chromium - is also present in the chemical composition to ensure corrosion resistance at all temperature, it was wished to take the same atomic content in tantalum as the one in carbon in order to avoid the formation of chromium carbides. With this choice, to 1 wt.% of carbon corresponds 15 wt.% of tantalum, which is already a very high content in such element. It was then chosen to limit the carbon content to 1 wt.% and then the tantalum one to 15 wt.%. An alloy Co(bal.)-30Cr-1C-15Ta was then elaborated and characterized in terms of as-cast microstructure, hardness and oxidation behaviour at high temperature, this after preliminary thermodynamic calculations to verify the interest of such composition.

EXPERIMENTAL

Preliminarily to the real elaboration, previsions about the development of the microstructure during solidification were done by using the Thermo-Calc version N software[9] and a database initially containing the descriptions of the Co-Cr-C system and its sub-systems[10-15] enriched by the description of the binary and ternary sub-systems Ta-C, Co-Ta, Cr-Ta and Co-Ta-C[16-18]. The successive appearance (and disappearance) of the different phases were characterized (temperatures), the theoretic mass fractions and the chemical compositions of the different phases were plotted versus temperature from the liquidus down to 500°C (temperature at which one can consider for such system that diffusion is too slow to allow the real microstructure still well fitting the theoretical one.

The quaternary Co-30Cr-1C-15Ta alloy (all contents in weight percents) was elaborated by foundry under inert atmosphere (pure Argon, 300mbars before heating, by melting together pure elements (Co, Cr and Ta: Alfa Aesar, purity higher than 99.9 wt.%; C: graphite), using a CELES high frequency induction furnace. Melting and solidification were achieved in the water–cooled copper crucible of the HF furnace to obtain an ingot of about forty grams. It was thereafter cut to obtain a first sample for the metallographic examination and the hardness characterization (Testwell Wolpert apparatus with Vickers indentor, load 30kg) of the as-cast microstructure, and a second one to be exposed at high temperature during 46h at 1150°C in the laboratory air in a resistive tubular furnace (after surface preparation: polished with 1200-grade SiC paper). The heating to the stage temperature (1150°C) was realized at +20°C min^{-1} and the cooling after the stage was done in the furnace itself, then slowly.

The as-cast sample as well as the sample exposed during 46h at 1150°C in air (after preliminary electrolytic Ni-coating for oxide scale protection and cutting) were embedded in a cold resin mixture (manufacturer ESCIL: resin CY230 + hardener HY956) and polished with SiC papers from 240 to 1200 grit. The final polishing was done by using a textile disk enriched with 1µm alumina particles. The metallographic observations were carried out using a Scanning Electron Microscopy (SEM JEOL JSM-6010LA), in the Back Scattered Electrons mode (BSE) with an acceleration voltage of 20kV, with special attention to the bulk microstructure of the as-cast alloy and to the oxide scale and alloy sub-surface for the sample exposed to high temperature.

RESULTS AND DISCUSSION

Thermodynamic calculations

Calculations of the successive stable states were carried out with Thermo-Calc and the results are graphically presented in Figure 1.

Solidification starts at 1444°C (liquidus temperature) with the appearance of the FCC TaC carbide phase. TaC grows from 0 to 4.10 mass.% during the cooling down to 1307°C, temperature at which the second solid phase appears: the FCC matrix of cobalt, which develops quickly since before the final solidification of additional TaC phase and cobalt matrix (eutectic) at 1296°C (solidus temperature). During the solid state cooling a third phase appears at 1168°C - the

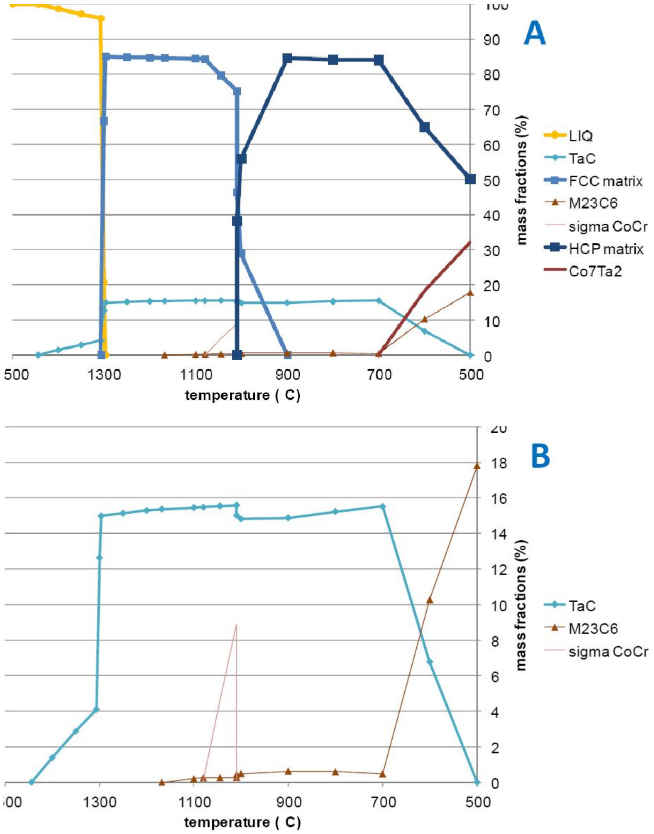

Figure 1 : Development of the microstructure of the Co-30Cr-1C-15Ta alloy during solidification, according to Thermo-Calc (B: enlargement of the low mass fractions part of A)

$M_{23}C_6$ chromium carbides – followed by a sigma phase Co_xCr at 1080°C which thereafter disappears at 1009°C at the same time of the crystallization of the HCP Co matrix. The later one progressively replaces the high temperature austenitic Co matrix from 1009°C down to near 900°C, and the matrix is now only hexagonal at low temperatures. However, bellow 700°C, a part of this HCP Co matrix is partly replaced by a sigma phase while, at the same time, the tantalum TaC phase is replaced by an intermetallic compound Co_7Ta_2. If, at 500°C, only one half of matrix is replaced by the sigma phase, TaC is wholly replaced by the intermetallic compound at the same temperature, and by the chromium carbide $M_{23}C_6$.

During solidification the chemical composition changes a little, as graphically shown in Figure 2.

Due to the growth of the TaC phase the tantalum and carbon contents in the liquid decrease (from 1 to 0.78 wt.% and from 15 to 11.65 wt.% respectively) while consequently the cobalt and chromium increases (from 54 to 56.31 wt.% and from 30 to 31.27wt.% respectively). During the eutectic solidification (rest of liquid → TaC + FCC Co matrix) there is an inversion in the evolution of the liquid contents in Co (52.67 wt.% at the solidus) and in carbon (0.98 wt.% at the solidus) while the liquid contents in Cr and in Ta keep on increasing (to 37 wt.%) and decreasing (to 9.35 wt.%) respectively.

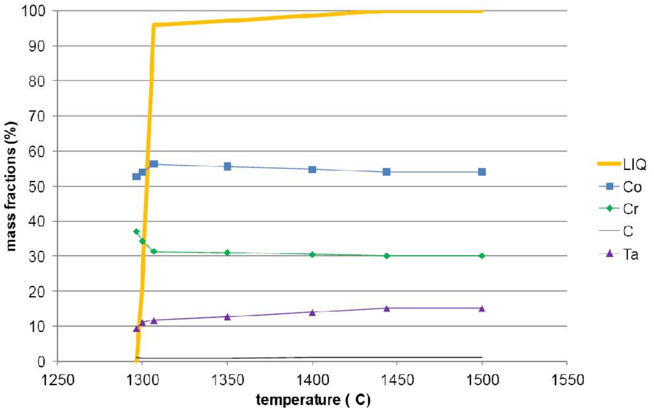

Figure 2 : Evolution of the mass fraction and of the chemical composition of the liquid phase during the cooling until its disappearance (according to Thermo-Calc)

The composition of the TaC phase (Figure 3) and of the $M_{23}C_6$ one (Figure 4) vary just a little with, for the first carbide, weight contents in Ta, C and also Cr and Co evaluating in the [93.49; 93.76], [6.16; 6.22], [0.02; 0.3] and [0; 0.03] ranges respectively, and for the second carbide, weight contents in Cr, C and also Co evaluating in the [80.35; 83.08], [5.59; 5.61] and [11.32; 14.07] ranges respectively (the Ta content being constantly zero.

The variations of the chemical compositions of the FCC Co matrix (Figure 5) and of the HCP Co one

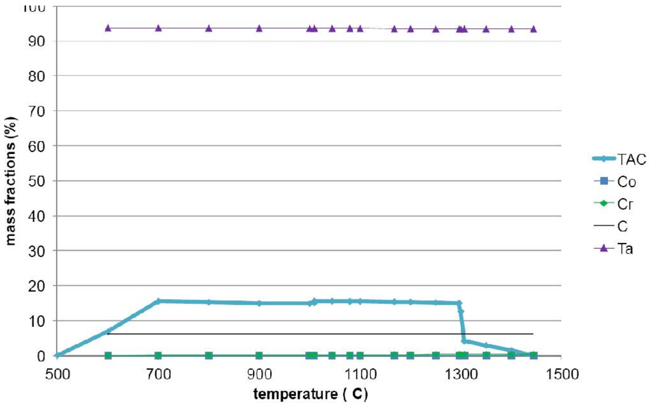

Figure 3 : Evolution of the mass fraction and of the chemical composition of the TaC phase during the cooling until its disappearance (according to Thermo-Calc)

(Figure 6) are more interesting to follow. During the cooling the Cr content in the FCC Co matrix begins to increase (from 31.75 to 35.41 wt.% between 1306.72°C and 1167.79°C) then it slightly decreases down to 32.79wt.% at 1000°C before the disappearance of the phase. In the same time the contents on C and in Ta continuously decrease from 0.08 to 0.02 and from 1.54 to 0.52 wt.% at 1000°C, with consequently a first decrease followed by an increase for the base element Co. The HCP appears at 1009.39°C and develops with contents varying as follows: Cr decreases from 36.86 down to 30.26 wt.%, C decreases from 0.09 down to 0 and Ta decreases from 1.80 down to 0.12 wt.%, between the temperature of HCP appearance (1009.39°C) and 500°C.

The chemical compositions of the sigma phase (CoCr) and of the intermetallic compound (Co_7Ta_2) do not vary significantly over their temperature ranges of existence (for Sigma; for Co_7Ta_2: calculations not done under 500°C).

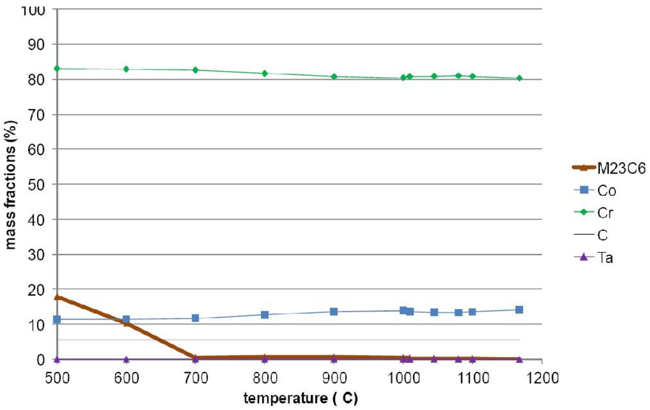

Figure 4 : Evolution of the mass fraction and of the chemical composition of the $M_{23}C_6$ phase during the cooling down to 500°C (according to Thermo-Calc)

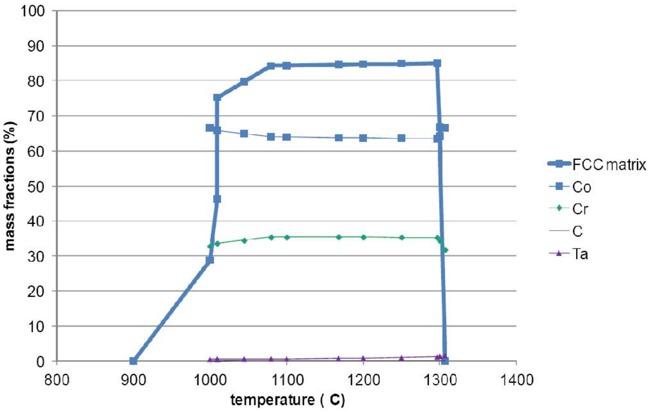

Figure 5 : Evolution of the mass fraction and of the chemical composition of the FCC matrix phase during the cooling down to its disappearance (according to Thermo-Calc)

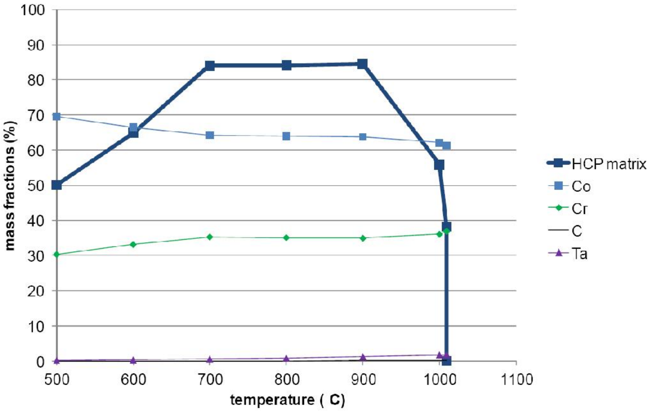

Figure 6 : Evolution of the mass fraction and of the chemical composition of the HCP matrix phase during the cooling down to its disappearance (according to Thermo-Calc)

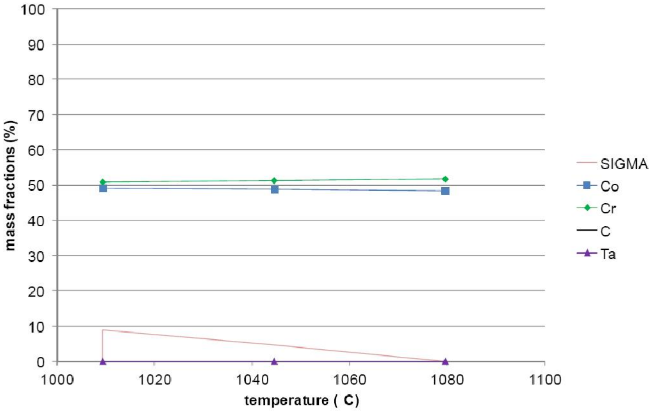

Figure 7 : Evolution of the mass fraction and of the chemical composition of the Sigma phase during its short existence (according to Thermo-Calc)

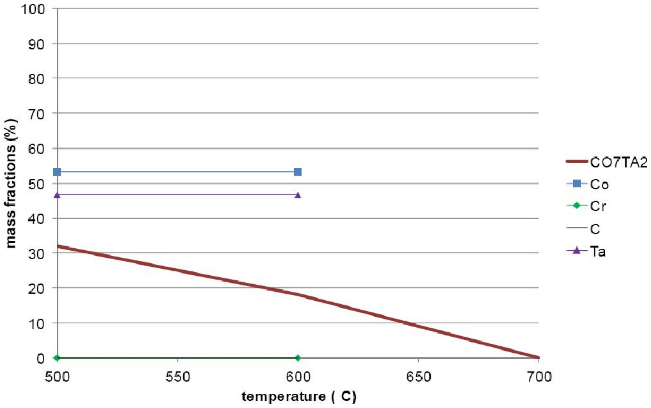

Figure 8 : Evolution of the mass fraction and of the chemical composition of the Co_7Ta_2 intermetallic compound during its short existence (according to Thermo-Calc)

The obtained as-cast microstructure

The microstructure of the studied Co-30Cr-1C-

15Ta alloy just after solidification and cooling down to room temperature is illustrated by the micrograph presented in Figure 9, with the global chemical composition of the alloys as determined by EDS in the centre of the ingot. This general composition is in rather good agreement with what was targeted before elaboration, except the tantalum content which is sensibly lower than expected. The matrix is dendritic and there is a white phase being mainly of eutectic type (with matrix) and situated in the interdendritic spaces while other white particles, more compact, are also present. Several pinpoint EDS measurements were performed in the microstructures (Figure 10). This revealed that the white phase is TaC, as clearly identified on the coarsest ones, but which is also extremely probable for the script-like interdendritic eutectic particles. The matrix contain more than 30wt.% of chromium due to a significant volume fraction occupied by the TaC phase which contains only little amount of chromium, as well as a significant part of tantalum (more than 3 wt.%), in solid solution too.

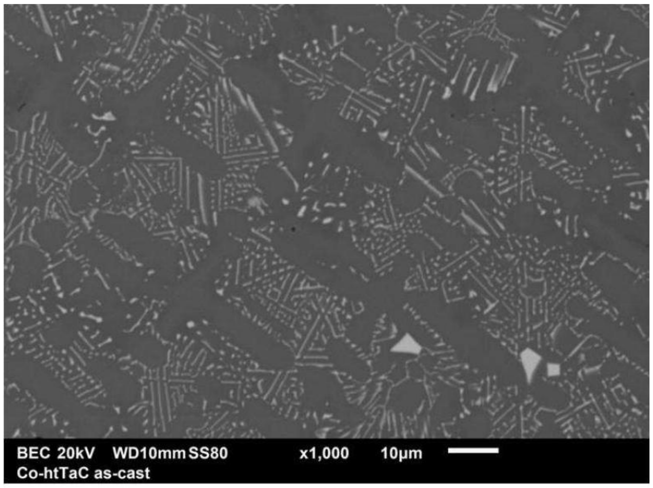

General composition: 55.45Co-32.10Cr-12.45Ta+C (wt.%)

Figure 9 : The as-cast microstructure of the Co-30Cr-1C-15Ta and the obtained general chemical composition of the alloy (SEM/BSE micrograph)

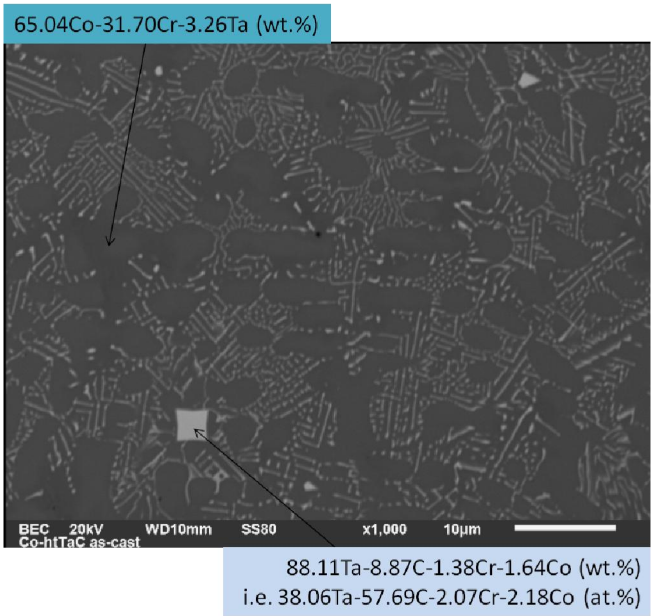
65.04Co-31.70Cr-3.26Ta (wt.%)

88.11Ta-8.87C-1.38Cr-1.64Co (wt.%)
i.e. 38.06Ta-57.69C-2.07Cr-2.18Co (at.%)

Figure 10 : Some results of matrix chemical composition and of particles identification (SEM/EDS measurements)

The external part of the ingot presents an external microstructure which appears very particular: there is a very dense population of compact TaC carbides isolated from one another rather confined zones of Co-based matrix containing also tantalum (about 2 wt.%Ta) but very rich in chromium (more than 40 wt.%Cr).

The same mounted as-cast sample was tested in Vickers hardness, this leading to the values presented in TABLE 1. The three obtained values are all higher than 400 Hv and rather close to one another, this leading to an average hardness of about 435.

TABLE 1 : Results of Vickers indentations on the as-cast alloy (load: 30 kg)

Individual values	Average hardness	Standard deviation
434 – 429 - 444	436	8

Behaviour in high temperature oxidation

The surface state of the sample exposed to the laboratory air during 46 hours at 1150°C in the tubular furnace is illustrated by the SEM/BSE micrograph presented in Figure 12. As this sample was cut in the core of the ingot its chemical composition and its initial microstructures were of the Figure 9 type. One can see that an external oxide obviously developed all over the sample, but the most part of this one was lost during the cooling, and only some isolated parts were available for further characterization. It is in addition possible to see that internal oxidation also occurred in the subsurface with the appearance of a dense population of pale oxides, and that a carbide-free zone developed from the {external oxide / alloy} interface.

Some EDS pinpoint results were acquired on the different types of oxides and a series of EDS pinpoints measurements was performed in the sub-surface at an increasing depth from the oxide/alloy interface. The locations of all these pinpoint measurements are shown

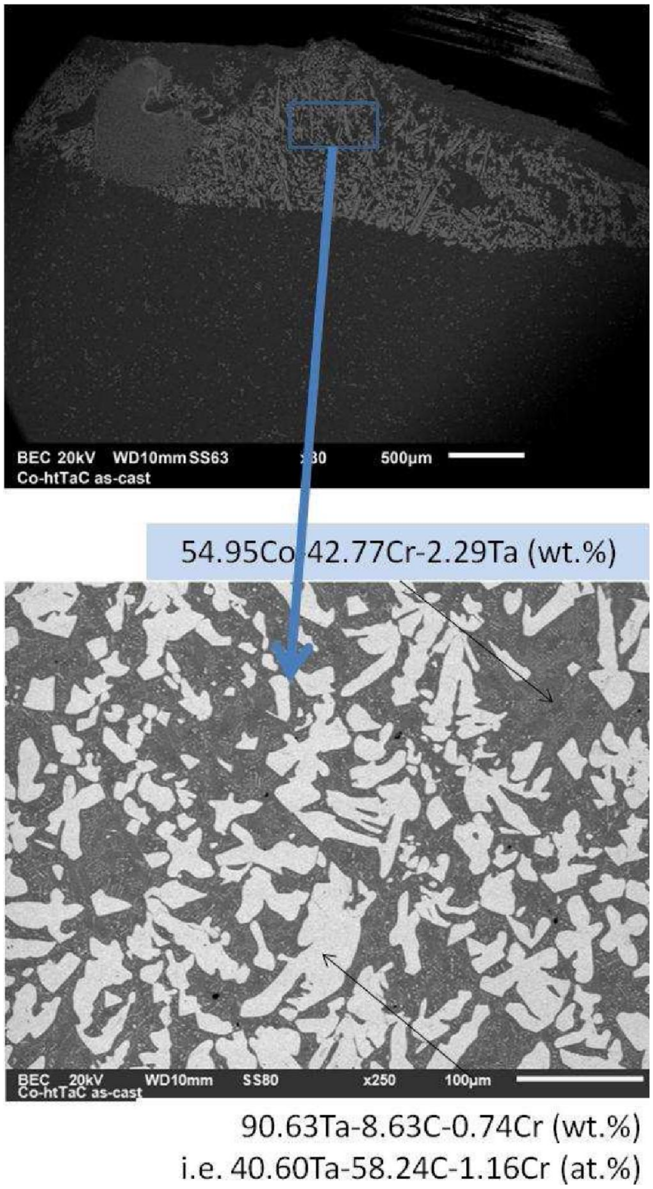

Figure 11 : Aspect of the external part of the ingot and pinpoint chemical analysis of this special zone (SEM/BSE and SEM/EDS measurements)

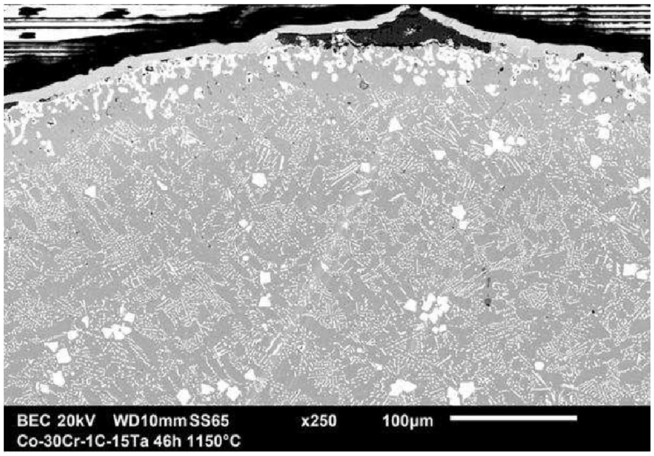

Figure 12 : General aspect of the external surface of the sample after exposure to laboratory air at 1150°C during 46 hours (SEM/BSE micrograph)

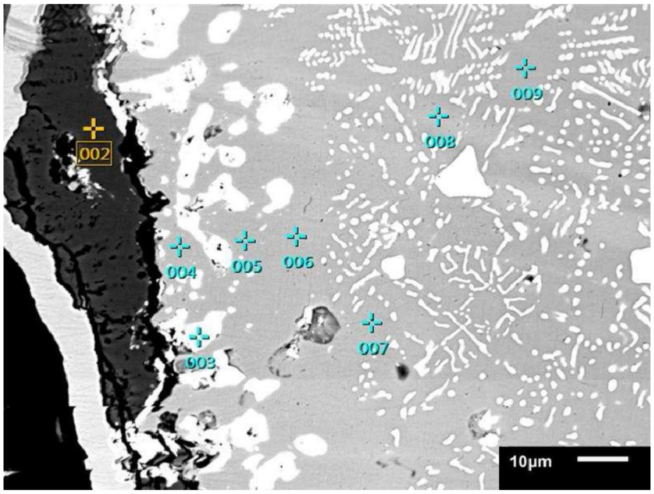

Figure 13 : Locations of the EDS measurements (EDS/BSE micrograph)

TABLE 2 : Chemical composition of the two types of oxides formed on surface and in the subsurface; locations numbered according to Figure 13

Oxides' compositions in at.% (and wt.%)	O	Cr	Ta	Co
002	63.43 at.% (34.59 wt.%)	36.27 at.% (64.28 wt.%)	0.13 at.% (0.80 wt.%)	0.16 at.% (0.33 wt.%)
003	60.86 at.% (17.41 wt.%)	16.33 at.% (15.19 wt.%)	19.87 at.% (64.30 wt.%)	2.94 at.% (3.10 wt.%)

in the micrograph given in Figure 13 and the obtained results are displayed in TABLE 2 (oxides) and TABLE 3 (sub-surface).

It appears that the dark oxide is chromia (Cr_2O_3) and the pale ones are oxides of both chromium and tantalum ($CrTaO_4$), as easily deduced from the results of TABLE 2 (respectively points '002' and '003'). In extreme surface the chromium content has fallen down to a little more than 22wt.% and the tantalum content down to about 0.6 wt.%. By penetrating deeper in the alloy the contents in both elements increase. The chromium content is equal again to the bulk value at about 70µm from the extreme surface while the tantalum content seems reaching a maximum value (about 1.5 wt.%) at a depth equal to 35 µm, as is to say at the boundary separating the carbide-free zone and the more internal

TABLE 3 : Evolution of the local chemical composition with the depth from extreme surface (EDS pinpoint analysis); locations numbered according to Figure 13

004	005	006	007	008	009	Element (wt.%)
22.19	22.59	23.97	24.99	29.97	32.87	Cr
0.61	0.49	1.39	1.49	1.37	1.11	Ta
77.19	76.92	74.63	73.52	68.66	66.02	Co

zone where the TaC carbides are still present. Deeper it seems decreasing down to 1 wt.%.

General commentaries

Increasing the carbon content and the tantalum one up to so high values, 1wt.% for C and 15 wt.% for Ta, the obtained microstructure remains analogous to the ones of TaC-strengthened superalloys: equi-axed dendritic matrix and script-like carbides mixed with matrix in the interdendritic spaces. However there is a little difference in the microstructure – the presence of compact TaC particles – which reveals a fundamental difference about the solidification scenario – TaC is the first solid to crystallize (instead matrix) – which was suspected by looking to the preliminary thermodynamic calculations. Indeed, Thermo-Calc showed this pro-eutectic TaC crystallization – over a particularly wide temperature range (about 300°C) – which can be considered as being at the origin of a continuous migration of the formed compact carbides toward the external zone of the molten liquid. Such phenomenon was previously encountered for pro-eutectic chromium carbides in cobalt-30wt.%Cr very rich in carbon (2.5wt.% and more)[19] and for pro-eutectic hafnium carbides in carbon containing cobalt-25wt.%Cr rich in hafnium (3.7 and 7.4 wt.%)[20]. Thus, the previsions done with Thermo-Calc calculations, which can be valuable if such displacement of the earliest TaC particles caused by the electromagnetic stirring does not occur, are necessarily not correct (except of course the evidencing of this pro-eutectic TaC crystallization). However these calculated results are available for describing the mass fraction evolution aspect of the microstructure development during slow solidification and solid state cooling.

The loss of the migrated first crystallized TaC carbides is not followed by the eventual one of the eutectic TaC carbides since these ones are necessarily interlocked with the dendrites and are then not so movable even when the alloy is still in mushy state. However, the chemical composition of the centre of the ingot is impoverished in tantalum (as evidenced by EDS) and probably too in carbon (too light element to be specified with EDS in weight content). One can guess that the eutectic part of TaC carbides (representing about 11% of the alloy in mass according to Thermo-Calc) has not suffered from this pro-eutectic TaC migration, but the hardness may be significantly diminished because of the loss of the pro-eutectic TaC (representing about 4% of the alloy in mass according to Thermo-Calc, as is to say the quarter of the whole TaC quantity). The hardness, which is just a little higher than the one of Co-30Cr-xC alloys with the same carbon content (x=1wt.%)[21], which is hardened by the presence of between 15 and 20mass.% of $M_{23}C_6$, is finally not so decreased.

The exposure to high temperature, even realized during a rather long time (46 hours) and at a particularly high temperature (1150°C) for friction applications did not induce neither a severe surface degradation (alloy still showing a chromia-forming behaviour) nor a microstructure degradation (the interdendritic carbides are just a little fragmented). This is a rather good surprise for an alloy so charged in such an oxidable element as tantalum. The only effect of this high content in tantalum is obviously the particularly high amount of internal $CrTaO_4$ oxide in the thin sub-surface.

CONCLUSIONS

Thus, with so high contents in carbon and especially in tantalum, a dense population of carbides – exclusively of TaC – was obtained. Their interdendritic repartition as well as their script-like form and mixing with matrix, guarantee good mechanical behaviour at medium and high temperatures. The room temperature hardness is rather high but it may be enhanced for better wear resistance, for example by increasing again the carbon and tantalum contents. This should not threaten the high temperature oxidation resistance – a property also very important – since with already so high content in a very oxidable element (15wt.%Ta) the behaviour of the alloy studied here was good and even after 46 hours at the rather high temperature of 1150°C, the alloy was still chromia-forming with in addition a chromium content on extreme surface not decreased to a critical value.

REFERENCES

[1] D.A.Bridgeport, W.A.Brandtley, P.F.Herman; Journal of Prosthodontics, **2**, 144 **(1993)**.

[2] C.T.Sims, W.C.Hagel; The superalloys, John Wiley & Sons, New York, **(1972)**.

[3] P.Berthod, J.L.Bernard, C.Liébaut; Patent WO99/16919.

[4] P.Kofstad; High Temperature Corrosion, Elsevier applied science, London, **(1988)**.

[5] E.F.Bradley; Superalloys: A Technical Guide, ASM International, Metals Park, **(1988)**.

[6] B.Roebuck, E.A.Almond; Int.Mater.Rev., **33**, 90 **(1988)**.

[7] A.Klimpel, L.A.Dobrzanski, A.Lisiecki, D.Janicki; J.Mater.Process.Tech., **164,165**, 1068 **(2005).**

[8] P.Berthod, O.Hestin, E.Souaillat; Materials Science: An Indian Journal, **7(1)**, 59 **(2011)**.

[9] Thermo-Calc version N: Foundation for Computational Thermodynamics, Stockholm, Sweden, Copyright, **(1993,2000)**.

[10] A.Fernandez Guillermet; Int. J Thermophys., **8**, 481 **(1987)**.

[11] J.O.Andersson; Int.J.Thermophys., **6**, 411 **(1985)**.

[12] P.Gustafson; Carbon, **24**, 169 **(1986)**.

[13] A.Fernandez Guillermet; Z.Metallkde, **78**, 700 **(1987)**.

[14] J.O.Andersson; Calphad, **11**, 271 **(1987)**.

[15] A.Fernandez Guillermet; Z.Metallkde., **79**, 317 **(1988)**.

[16] K.Frisk, A.Fernandez Guillermet; J.Alloys Compounds, **238**, 167 **(1996)**.

[17] Z.K.Liu, Y.Austin Chang; Calphad, **23**, 339 **(1999)**.

[18] N.Dupin, I.Ansara ; J.Phase Equilibria, **14**, 451 **(1993)**.

[19] P.Berthod, O.Hestin, E.Souaillat; Materials Science: An Indian Journal, **7(1)**, 59 **(2011)**.

[20] P.Berthod; Materials Science: An Indian Journal, **9(11)**, 420 **(2013)**.

[21] P.Berthod; Materials Science and Technology, **25(5)**, 663 **(2009)**.